Huang et al. *Zool. Res.* 2025, 46(6): 1488−1500
https://doi.org/10.24272/j.issn.2095-8137.2025.106
https://cstr.cn/32248.14.zr.2025.106

ZR | Zoological Research

Article Open Access

Regulation of UBC12 expression and protein neddylation by PINK1 suggests a primate-specific function

Wei Huang[1], Ting Xu[1], Gong-Ke Zhou[1], Yu-Xuan Li[1], Chuang-Zhen Lin[2], Xiu-Sheng Chen[1], Tong Zhang[1], Liang Jiang[1], Yan-Ting Liu[1], Xin Xiong[1], Xue-Ying Liang[1], Xiang-Yu Guo[1], Shi-Hua Li[1], Xiao-Jiang Li[1,3], Wei-Li Yang[1,*]

[1] *Guangdong Key Laboratory of Non-human Primate Research*, *Key Laboratory of CNS Regeneration (Ministry of Education)*, *GHM Institute of CNS Regeneration*, *Jinan University*, *Guangzhou*, *Guangdong* 510632, *China*

[2] *Department of Gastroenterology*, *Third Affiliated Hospital of Guangzhou Medical University*, *Guangzhou*, *Guangdong* 510150, *China*

[3] *Lingang Laboratory*, *Shanghai* 200031, *China*

ABSTRACT

Mutations in PTEN-induced putative kinase 1 (*PINK1*) are implicated in early-onset Parkinson's disease (PD). Despite various *in vitro* studies indicating the importance of PINK1 in mitophagy, its physiological function in the brain remains poorly defined due to undetectable protein levels in rodents and cultured cells under basal conditions. Here, PINK1 was found to be selectively expressed in the primate brain, enabling exploration of its endogenous role *in vivo*. Proteomic profiling via mass spectrometry identified the ubiquitin-conjugating enzyme E2M (UBC12) as a PINK1-interacting partner, with strong colocalization in the monkey brain. Knockdown of *PINK1* in monkeys resulted in marked reductions in UBC12 protein abundance and global neddylation, effects not observed in brain tissues from *PINK1* knockout mice or pigs. These findings reveal a primate-specific PINK1-UBC12 axis and uncover a previously unrecognized role for PINK1 in protein neddylation, distinct from its established mitophagy function.

Keywords: PINK1; UBC12; Monkey model; Neddylation; Parkinson's disease

INTRODUCTION

Biallelic mutations in PTEN-induced putative kinase 1 (*PINK1*) and *Parkin* are causally linked to early-onset Parkinson's disease (PD). *PINK1* encodes a mitochondrial serine/threonine kinase that, under stress conditions, phosphorylates both Parkin and ubiquitin at Ser65, subsequently facilitating the clearance of damaged mitochondria through mitophagy (Chu, 2019; de Vries & Przedborski, 2013; Eldeeb & Ragheb, 2020; Liu et al., 2020; Pickrell et al., 2015; Pickrell & Youle, 2015). However, *in vivo* evidence substantiating this pathway remains scarce, in part because endogenous PINK1 is nearly undetectable under basal conditions in rodent tissues and standard cell lines (Akundi et al., 2011; Gispert et al., 2009), with detection requiring either immunoprecipitation enrichment (McWilliams et al., 2018) or artificial induction via acute mitochondrial depolarization (Narendra et al., 2010; Yamano & Youle, 2013). Furthermore, PINK1-deficient mouse and pig models fail to recapitulate the hallmark dopaminergic neurodegeneration seen in PD patients (Akundi et al., 2011; Gispert et al., 2009; Kitada et al., 2007; Wang et al., 2016, 2023; Xiong et al., 2009; Zhou et al., 2015). Even genome editing in non-human primates (NHPs) using single-strand nickases fails to abolish PINK1 protein expression or induce PD-associated phenotypes (Chen et al., 2021), underscoring the need for more precise models to study endogenous PINK1 function.

As reported in our previous study, PINK1 is abundantly expressed in the primate brain, with its deficiency resulting in severe neurodegeneration (Yang et al., 2019). Notably, this phenotype arises without substantial disruption to mitochondrial homeostasis, implicating alternative kinase-dependent pathways (Chen et al., 2024; Yang et al., 2022). Although *in vitro* studies have identified that PINK1 phosphorylates Parkin, the lack of PINK1 protein in rodent models has prevented *in vivo* validation (Gladkova et al., 2018; Kane et al., 2014; Koyano et al., 2014). Using NHP models, phosphorylation of endogenous Parkin by PINK1 has been demonstrated, a crucial step for reducing toxic alpha-synuclein accumulation (Han et al., 2024). Furthermore, phosphorylated PINK1 substrates are readily detected in

Received: 24 April 2025; Accepted: 12 May 2025; Online: 13 May 2025

Foundation items: This work was supported by the National Key Research and Development Program of China (2021YFF0702201), National Natural Science Foundation of China (32070534, 32370567, 81830032, 31872779, 82071421, 81873736), Department of Science and Technology of Guangdong Province (2021ZT09Y007, 2020B121201006), Guangdong Basic and Applied Basic Research Foundation (2023B1515020031, 2022A1515012301), K.C. Wong Education Foundation, Fundamental Research Funds for the Central Universities (Jinan University, 11620358) and Hubei Topgene Biotechnology Co. Ltd.

*Corresponding author, E-mail: weiliyang12@jnu.edu.cn

monkey brains but remain absent in tissues from mice and pigs lacking detectable PINK1 (Chen et al., 2024). These findings collectively underscore the importance of NHP models for elucidating the physiological functions of PINK1.

Emerging evidence suggests that PINK1 operates beyond mitochondrial surveillance. In primates, subcellular localization studies have reported that PINK1 and Parkin distribute independently and only converge within mitochondria under acute stress (Liu et al., 2025), suggesting distinct functional roles under normal conditions. PINK1 is also involved in tumorigenesis and cancer development (Arena & Valente, 2017; O'Flanagan & O'Neill, 2014), further supporting a broader regulatory repertoire.

Given the species-specific expression profile of PINK1, NHPs offer a critical model for exploring its *in vivo* interactome and functional landscape. To investigate endogenous PINK1-associated signaling under physiological conditions, this study identified PINK1-interacting proteins in the primate brain. Mass spectrometry revealed that PINK1 is associated with UBC12, an E2-conjugating enzyme involved in the NEDD8 modification pathway (Choo et al., 2012). NEDD8-mediated neddylation plays a central role in neuronal development and maintenance (Ayuso-García et al., 2024; Vogl et al., 2015) and has been linked to the etiology of neurodegenerative disorders (Chen et al., 2012; Govindarajulu et al., 2022; Saurat et al., 2024; Zhang et al., 2024) and tumorigenesis (Liu et al., 2024; Zhang et al., 2024; Zheng et al., 2021). In primate brain tissue, PINK1 deficiency resulted in a marked reduction in UBC12 abundance and global neddylation levels, implicating PINK1 as a modulator of this post-translational modification. These findings expand the known functional scope of PINK1 beyond mitophagy, establishing a primate-specific regulatory axis that may inform new mechanistic insights into its physiological role.

MATERIALS AND METHODS

Antibodies

Antibodies were either obtained from commercial sources or previously generated in-house. The following were used: PINK1 (BC100-494, Novus Biologicals, USA; S086D, MRC PPU Reagents and Services, UK; E7B6, self-made; MAB 4357, Millipore, USA; 23707, self-made), NeuN (177487, Abcam, UK), Vinculin (MAB3574, Millipore, USA), RohB (GTX108600, GeneTEX, USA), PRDX1 (sc137222, Santa Cruz, USA), UBC12 (14520-1-AP, Proteintech, USA; SC390064, Santa Cruz, USA), Rab14 (sc271401, Santa Cruz, USA), ATP5A (ab110273, Abcam, UK), NEDD8 (ET1702-84, HUABIO, China), EEF1A1 (11402-1-AP, Proteintech, USA), and MBP (MAB386, Millipore, USA). Antibody dilutions were provided in Supplementary Table S1.

Plasmid constructs and transfection

Truncated GST-tagged PINK1 constructs were designed as illustrated in Figure 1C. The pGEX-4T1-GST-Δ155PINK1 vector was generated using cDNA from monkey brain and amplified with the following primers: forward 5′-CGGGATC ATCCATGTATCTGATAGGGCAGTCCATTG-3′, reverse 5′-C GGAATTCTCACAGGGCTGCCCTCCATGAG-3′. Polymerase chain reaction (PCR) products were cloned into the pGEX-4T1 plasmid and verified by sequencing prior to downstream applications. The plasmid was transformed into BL21(DE3) competent bacteria, heat-shocked at 55°C for 45 s, incubated on ice for 30 min, and plated on LB agar. After overnight incubation at 37°C, a single colony was selected for expansion in LB Broth (Beyotime, China). Plasmids were purified using plasmid purification kits (Magen, China).

GST pull-down assays

GST-tagged proteins were expressed in *Escherichia coli* BL21(DE3) using the pGEX 4T1 vector and induced with 1 mmol/L IPTG. Purified GST fusion proteins were incubated with glutathione Sepharose beads (Millipore, USA) at 4°C overnight. Bead-bound proteins were subjected to western blot analysis. For interaction assays, glutathione Sepharose beads were mixed with monkey cortical homogenates at a ratio of 5:1 and incubated at 4°C overnight. Beads were washed four times with RIPA buffer (Beyotime, China) at 1 000 r/min for 5 min at 4°C. Samples were collected from the last wash and boiled for western blot analysis. Coomassie Brilliant Blue staining (Beyotime, China) was performed according to manufacturer's instructions. Liquid chromatography-mass spectrometry (LC-MS) was conducted by Novogene Bioinformatics Technology (China).

Co-immunoprecipitation

Monkey cortical tissue was lysed in RIPA buffer (Beyotime, China) supplemented with protease and phosphatase inhibitors: Protease Inhibitor Cocktail (Thermo Fisher Scientific, USA), 5 mmol/L sodium fluoride (Sigma-Aldrich, Germany), 0.5 mmol/L sodium orthovanadate (Sigma-Aldrich, Germany), and 0.5 mmol/L phenylmethylsulfonyl fluoride (AMRESCO, USA). After homogenization and lysis, lysates were centrifuged at 10 000 r/min for 10 min at 4°C, and the supernatants were collected. Protein concentrations were determined by the BCA assay. Co-immunoprecipitation was performed using 2 mg/mL protein extracts incubated with 2–4 μg of antibody at 4℃ overnight. Immunocomplexes were recovered using 25 μL of protein G Sepharose (Thermo Fisher Scientific, USA), washed three times, and resolved by sodium dodecyl-sulfate polyacrylamide gel electrophoresis (SDS-PAGE), followed by electroblotting onto nitrocellulose membranes (Cytiva, USA).

Proximity ligation assay (PLA)

PLA was performed using a Duolink *in situ* proximity ligation assay reagent (Sigma-Aldrich, Germany) according to the manufacturer's instructions. Cells were plated onto 12-well chamber slides, washed with ice-cold phosphate-buffered saline (PBS) and methanol for 10 min at −20°C, and permeabilized using 0.1% Triton X-100. Following a series of additional washes and a 30 min blocking step in 3% BSA, primary antibodies were applied and incubated at 37°C for 2 h. PLA probes were added and incubated for 1 h at 37°C, followed by three washes. Ligation was performed at 37°C for 30 min, and amplification was carried out using polymerase solution. Nuclei were stained with 4',6-diamidino-2-phenylindole (DAPI). Images were acquired using an Olympus FV3000 laser confocal microscope (Japan) and analyzed using ImageJ software v.1.54p.

Primary cultured monkey neurons and astrocytes

To culture primary astrocytes, cortical tissue was isolated from 70-day monkey embryos and meninges were removed. Tissue was mechanically minced, washed with PBS, and enzymatically digested in 5 mL of 0.01 g/mL papain (Worthington, USA) and DNase I (1:50) at 37°C for 20 min with pipetting every 5 min. Cells were centrifuged at 300 ×*g* for

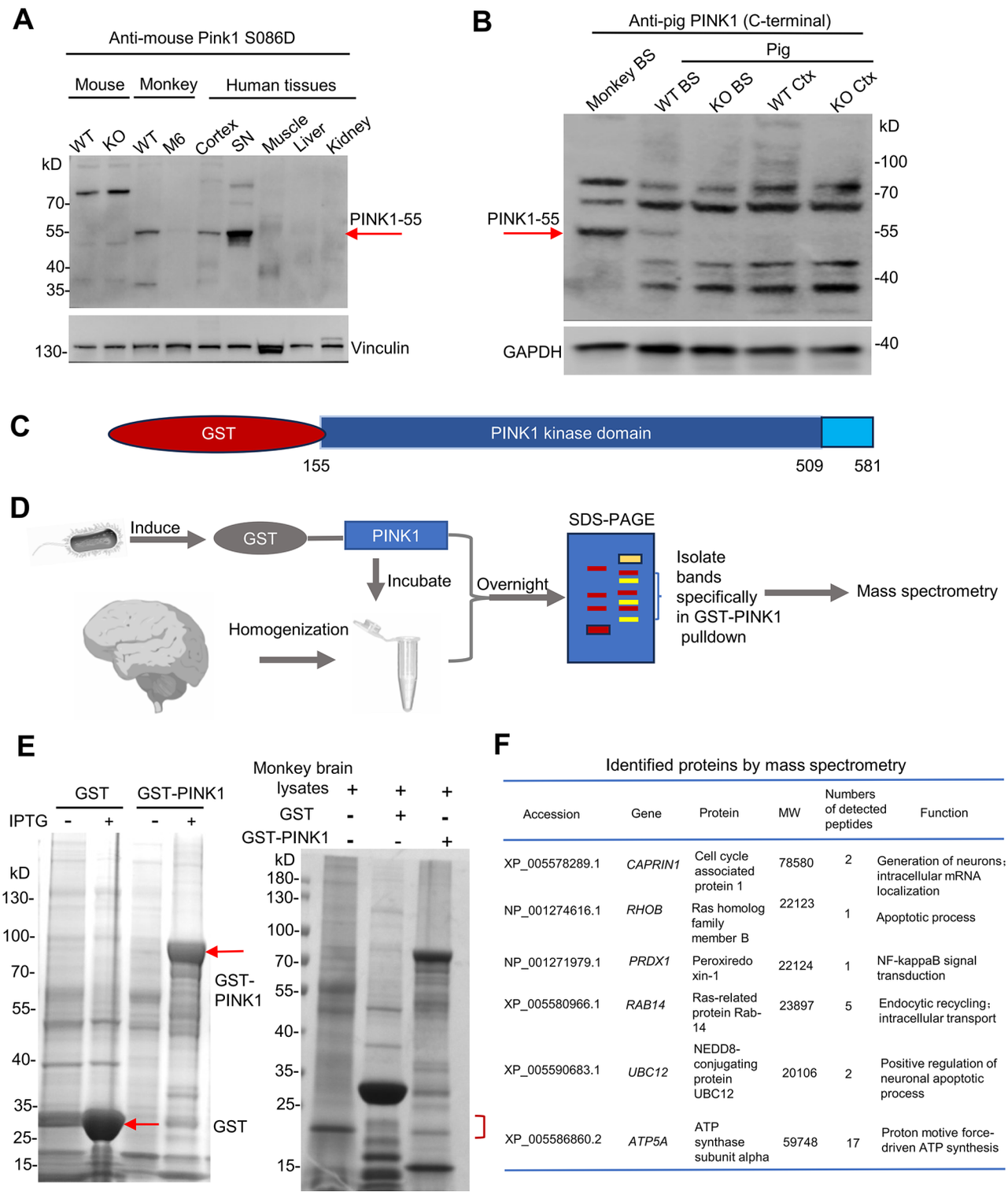

Accession	Gene	Protein	MW	Numbers of detected peptides	Function
XP_005578289.1	*CAPRIN1*	Cell cycle associated protein 1	78580	2	Generation of neurons; intracellular mRNA localization
NP_001274616.1	*RHOB*	Ras homolog family member B	22123	1	Apoptotic process
NP_001271979.1	*PRDX1*	Peroxiredoxin-1	22124	1	NF-kappaB signal transduction
XP_005580966.1	*RAB14*	Ras-related protein Rab-14	23897	5	Endocytic recycling; intracellular transport
XP_005590683.1	*UBC12*	NEDD8-conjugating protein UBC12	20106	2	Positive regulation of neuronal apoptotic process
XP_005586860.2	*ATP5A*	ATP synthase subunit alpha	59748	17	Proton motive force-driven ATP synthesis

Figure 1 Identification of PINK1-interacting proteins in the monkey brain using GST-pull-down assay

A: Western blot analysis of cortical tissues from 4-month-old wild-type (WT) and *Pink1* knockout (KO) mice, 3-year-old WT and *PINK1* mutant (M6) monkeys, and 54-year-old postmortem human samples from the brain cortex, substantia nigra (SN), muscle, liver, and kidney. Detection was performed using anti-mouse Pink1 S086D antibody (residues 175–250). PINK1-55 (red arrow) was selectively expressed in primate brain tissues and was reduced in the M6 monkey brain cortex. B: Western blot analysis of cortex (Ctx) and brainstem (BS) tissues from WT and *PINK1* KO pigs (postnatal day 1). BS tissue from a 3-year-old WT monkey served as a control to show PINK1 expression. Detection was performed using anti-pig PINK1 antibody (residues 484–504). PINK1-55 (red arrow) was detected in the monkey brain but not the pig brain. C: Schematic of the monkey GST-Δ155 PINK1 vector construct used for the pull-down assay. D: Experimental flowchart of GST pull-down assay. E: Coomassie Brilliant Blue staining of SDS-PAGE showing protein bands following incubation of purified GST or GST-Δ155 PINK1 with monkey brain lysates. GST and GST-Δ155 PINK1 bands are indicated by red arrows; red semicircular brackets indicate candidate PINK1-binding proteins. F: Selected candidate PINK1-interacting proteins identified by mass spectrometry.

5 min at room temperature, resuspended, and seeded onto poly-L-lysine-coated culture dishes (Sigma-Aldrich, Germany) in Dulbecco's Modified Eagle Medium (DMEM, Gibco, USA) supplemented with 10% fetal bovine serum (FBS, Gibco, USA) and 1% penicillin-streptomycin. After 24 h, the medium was replaced, and half-medium changes were carried out every 2–3 days.

For primary neurons, after initial adherence for 6 h to poly-L-lysine-coated culture dishes, the DMEM was replaced with Neurobasal medium (Gibco, USA) containing B27 supplement (Gibco, USA) and treated overnight with cytosine beta-D-arabinofuranoside crystalline (Arac, Sigma-Aldrich, Germany) to inhibit glial cell survival. Medium was refreshed every 2 days to maintain optimal culture conditions. Transfection of monkey astrocytes and neurons was carried out using a Cas9 plasmid and *PINK1*-targeting guide RNA (gRNA) plasmids with the Mouse Neural Stem Cell Nucleofector™ Kit (Lonza, Switzerland). The gRNA sequences targeting *PINK1* were: *PINK1* exon 2 sgRNA: 5′-GGCTGGAGGAGTATCTGATAggg-3′, *PINK1* exon 4 sgRNA: 5′-ccgGGTTCTCCGCGCTTTCACC-3′, and control gRNA: ACCGGAAGAGCGACCTCTTCT.

Human tissues

Postmortem brain and peripheral tissues were obtained from the Brain Bank of Xiangya School of Medicine via the willed body donation program. Samples from the prefrontal cortex, substantia nigra, brain stem, liver, muscle, and kidney were collected from a 54-year-old female donor who died of breast cancer. These tissues were used for western blot analysis. The use of postmortem human tissues was approved by the Institutional Ethics Committee of Central South University (Approval No. 2021-KT20, 10 March 2021), in compliance with the Code of Ethics of the World Medical Association (Declaration of Helsinki).

Animals

Generation of *PINK1*-mutant rhesus monkeys via embryonic microinjection and stereotaxic CRISPR/Cas9 delivery followed previously published protocols (Yang et al., 2015, 2019, 2022; Tu et al., 2017). All procedures were approved by the Institutional Animal Care and Use Committee at Guangdong Landao Biotechnology (China). The study was conducted in strict compliance with the "Guide for the Care and Use of Laboratory Animals of the Institute of Laboratory Animal Science (est. 2006)" and "The Use of Non-Human Primates in Research of the Institute of Laboratory Animal Science (est. 2006)" to ensure personnel safety and animal welfare. The genotypes and ages of the monkeys used in this study are provided in Table 1.

Pink1 knockout mice were generated by Beijing Biocytogen (China). Briefly, gRNAs were designed to target exons 2 and 4 of the mouse *Pink1* gene. *Cas9* mRNA and gRNAs were co-injected into C57BL/6 zygotes. F0 generation mice were genotyped using the following PCR primers: sense 5′-CTCC CCACTCTTGTGTTTGCTATGT-3′ and antisense 5′-CAGTT GCTGCTCAGAGTAGTTCACA-3′ for exon 2; sense 5′-CAC CATGTGAGATGGATAGATGGGC-3′ and antisense 5′-AAGT TAGCTGGCACTGAAAGAGGAC-3′ for exon 4. Mice carrying mutations in both alleles at exons 2 and 4 were designated as *Pink1* knockouts. All procedures involving animals were conducted in accordance with the Animal Care and Use Committee of Jinan University (Approval No. IACUC-20210220-06).

For *Ubc12* knockdown, 6–8-month-old wild-type (WT) mice were anesthetized with isoflurane, and placed in a stereotaxic apparatus (RWD, China). After a small scalp incision, the meninges were treated with 3% hydrogen peroxide and a cortical injection was made at coordinates ML: ±2.0, AP: 0, DV: –1.55 using AAV9-*Ubc12* shRNA virus or AAV9 scramble shRNA virus. After suturing, erythromycin ointment was applied, and mice were observed for 1 week. Brain tissues were collected 45 days post-injection for western blot analysis. *PINK1*-mutant and WT pig tissues were kindly provided by Prof. Jianguo Zhao. Details regarding pig model generation are provided in a previously published paper (Wang et al., 2016).

Immunofluorescent staining

Monkey brain tissue was perfused and fixed with 4% paraformaldehyde (PFA). Following initial 24 h fixation, samples were transferred to fresh 4% PFA for an additional 7 days. Fixed tissues were dehydrated sequentially in 15% and 30% sucrose until fully equilibrated, then embedded in optimal cutting temperature (OCT) compound. Sections were sliced at a thickness of 30 μm. For staining, slices were penetrated with 0.5% Triton X-100 in 1×PBS for 30 min and blocked with blocking buffer for 1 h at room temperature. Primary antibodies were applied and incubated overnight at 4°C. After three PBS washes, sections were incubated with secondary fluorescent antibodies for 1 h and DAPI for 10 min. Images were captured using a Zeiss Axiocam 506 color camera (Zeiss, Germany) or Olympus FV3000 confocal laser scanning microscope (Olympus, Japan). Fluorescence intensity and cell counts were quantified using ImageJ v.1.54p. The staining protocol for cultured neurons followed the same procedure.

Table 1 Monkeys used in this study

Name	Targeted gene	Sex	Death and age
M2	*PINK1* (germline knockdown (KD))	M	Postnatal day 7
M5	*PINK1* (germline KD)	M	1.5 years old (dead)
M6	*PINK1* (germline KD)	F	3 years old (euthanized)
M7	*PINK1* (germline KD)	M	Gestation day 139 (aborted)
KD1	*PINK1* (adult KD)	M	5 years old (euthanized)
KD2	*PINK1* (adult KD)	M	10 years old (euthanized)
Newborn WT	–	M	Postnatal day 140 (aborted)
WT	–	F	3 years old (euthanized)
WT-1	–	M	4.7 years old (euthanized)
WT-2	–	M	6 years old (euthanized)
WT-3	–	M	7 years old (euthanized)

M: Male. F: Female. –: Not available.

Western blot analysis

Tissue lysates were separated by SDS-PAGE and transferred to nitrocellulose (NC) membranes (Cytiva, USA). Membranes were blocked with 5% non-fat milk and incubated with primary antibodies at 4°C overnight. After washing, the membranes were incubated with corresponding secondary antibodies for 1 h at room temperature. The membranes were washed three times with TBST (10 min each), incubated with SuperSignal Chemiluminescent Substrate (CLINX, China), and scanned with the ChemiScope 6100BZ system (CLINX, China). Protein band densities were semi-quantified using ImageJ.

Reverse transcription-quantitative real-time PCR (RT-qPCR)

Total RNA was isolated from tissues or cultured cells using TRIzol reagent (Invitrogen, USA) according to the manufacturer's instructions. RNA concentration was determined using a NanoDrop spectrophotometer (Thermo Fisher Scientific, USA). Single-stranded cDNA was synthesized using a cDNA Synthesis Kit (Vazyme, China). Quantitative PCR (qPCR) was performed using SYBR Green Master Mix (Qiagen, Germany) and the CFX Touch system (Bio-Rad, USA). Gene expression levels were normalized to *ACTB* and calculated using the $2^{-\Delta\Delta Ct}$ method. Primer sequences included: PINK1 forward: CCATCGCCTATGA AATCTTTGGGCT, PINK1 reverse: CTCTTGCTGGCCTCTC GCTGGAGC; UBC12 forward: CATCTGTCCTGATGAGGGC TTC, UBC12 reverse: TGTCTCACACTTCACCTTGGG; ACTB forward: GAAGATCAAGATCATTGCTCCTC, ACTB reverse: CTGCTTGCTGATCCACATCTGCTG.

Quantification and statistical analyses

qPCR data were derived from three biological replicates per sample, and results were expressed as mean values. Western blot data were quantified by densitometry using ImageJ v.1.54p, and graphs were generated with GraphPad Prism v.8.02. The ratios of cDNA or proteins of interest to the internal (*ACTB*) or loading controls (Vinculin) were used for quantification. For western blots, replicates with comparable internal or loading controls were selected for quantification. Data are expressed as mean±standard error of the mean (SEM). Paired two-tailed *t*-tests were used to compare experimental and control groups. Statistical analysis was performed using GraphPad Prism v.8.02, and $P<0.05$ was used throughout this study to indicate significance.

RESULTS

Identification of PINK1-interacting proteins in the primate brain

Endogenous PINK1 is known to be intrinsically unstable *in vivo*, undergoing rapid degradation under basal conditions unless stabilized on depolarized mitochondria to initiate mitophagy (Beilina et al., 2005; Greene et al., 2012). As a result, detection of endogenous PINK1 protein has proven challenging in small animal brains, particularly rodents, under physiological conditions (McWilliams et al., 2018; Yang et al., 2022). However, recent studies have demonstrated that PINK1 is selectively and robustly expressed in primate brains, where it is essential for neuronal survival (Yang et al., 2019, 2022). To validate this primate-specific expression pattern, western blot analysis was performed using additional anti-PINK1 antibodies and brain tissues from *PINK1* knockout mouse and pig models, alongside postmortem human brain tissues. PINK1 protein was clearly detected in monkey and human brain tissues but remained undetectable in mouse and pig brains, even when using species-specific antibodies targeting mouse (Figure 1A) and pig (Figure 1B) PINK1 peptides.

To investigate endogenous PINK1 function in the primate brain, a proteomic screening was performed to identify proteins associated with PINK1. Initial attempts to immunoprecipitate native PINK1 using commercially available antibodies were unsuccessful, likely due to the membrane-associated distribution of PINK1 in the primate brain (Liu et al., 2025), which complicates its solubilization. To overcome this limitation, a GST-PINK1 fusion protein encompassing the kinase domain of monkey PINK1 was expressed in *E. coli* (Figure 1C) and used as bait to isolate interacting proteins from monkey brain lysates. The GST-PINK1 complexes were resolved by SDS-PAGE, and distinct bands specific to GST-PINK1 interactions were excised and subjected to mass spectrometry analysis (Figure 1D–F).

Proteins identified by mass spectrometry were subjected to functional enrichment analysis and protein-protein interaction (PPI) network analysis (Figure 2A). The size of each node represented the relative abundance of the identified proteins, with the top 15 candidates highlighted in yellow. Several high-confidence candidates (indicated by red arrows) were selected for validation using available antibodies. Using previously established *PINK1*-targeted monkey models (Yang et al., 2019, 2022), brain tissues were examined to identify PINK1-interacting proteins whose expression is altered in PINK1-deficient monkey brains, aiming to identify candidates with functional relevance to PINK1. Western blot analysis was performed to evaluate changes in the expression of RhoB, PRDX1, RAB14, UBC12, EEF1A1, MBP, and ATP5A. Among these, a notable reduction in UBC12, the ubiquitin-conjugating enzyme E2M, was observed in the cortex of PINK1-deficient monkeys (Figure 2B), as confirmed by densitometric quantification normalized to Vinculin (Figure 2C). A significant decrease in myelin basic protein (MBP), a key component of the myelination process in the nervous system, was also detected (Figure 2B). Given prior evidence that PINK1 deficiency induces neuronal cell death in the monkey brain (Yang et al., 2019, 2022), the observed down-regulation of MBP may reflect secondary effects of neurodegeneration. Expression of ATP5O and ARHGEF2B was additionally assessed; however, no clear bands were detected, likely due to low antibody specificity. Based on its consistent reduction and known role in neddylation, UBC12 was selected for further investigation.

Our previous studies demonstrated that PINK1 protein is abundantly expressed in primate brain tissue but remains undetectable or expressed at very low levels in peripheral tissues (Yang et al., 2022). Western blot analysis of tissues from monkeys and postmortem human donors revealed that UBC12 also exhibited brain-enriched expression compared to peripheral tissues (Figure 2D–F). UBC12 functions as a key component of the NEDD8-activating enzyme complex and plays a critical role in regulating neddylation (Enchev et al., 2015), a post-translational modification involved in neuronal development, synaptic plasticity, and the pathogenesis of neurodegenerative disorders such as Parkinson's disease (Ayuso-García et al., 2024; Govindarajulu et al., 2022; Vogl et al., 2015). Given its role as an E2-conjugating enzyme in the neddylation cascade and its enrichment in brain tissue, the

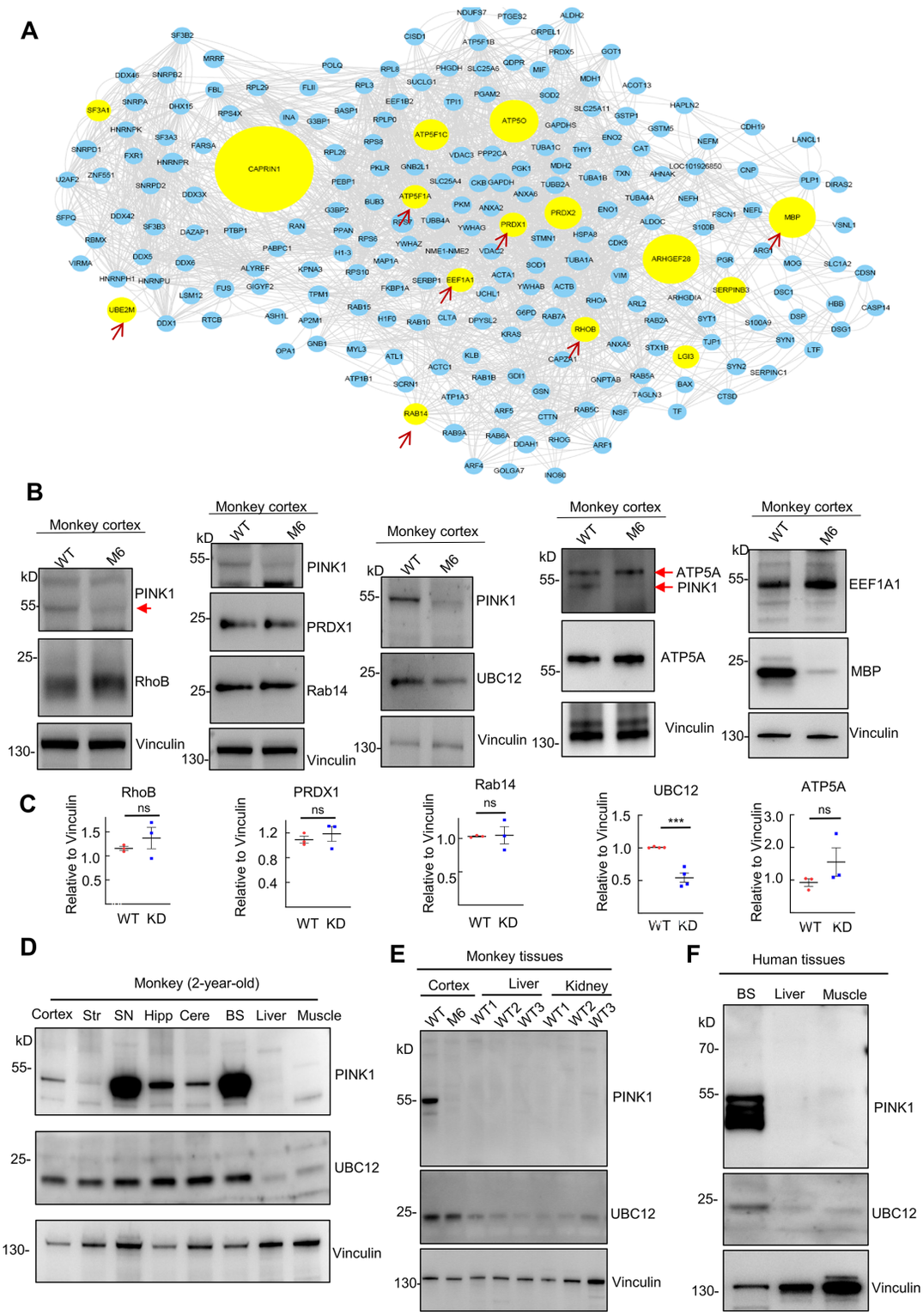

Figure 2 Identification of PINK1-interacting proteins down-regulated in the *PINK1* mutant monkey brain

A: Protein-protein interaction networks functional enrichment analysis (performed using STRING) of proteins interacting with GST-tagged PINK1 as identified by mass spectrometry. Circle size represents relative protein abundance, with yellow highlighted segment representing the top 15 candidate proteins. Proteins marked by red arrows (ATP5A, PRDX1, MBP, EEF1A1, RhoB, Rab14, and UBE2M) were selected for further validation using available antibodies. B: Western blot analysis of selected candidate proteins in brain cortex lysates from wild-type (WT, 3-year-old) and *PINK1*-knockdown (KD) (M6, 3-year-old) monkeys. UBC12 expression was markedly reduced following *PINK1* knockdown. Red arrows indicate positions of specific protein bands. C: Quantification of RhoB, PRDX1, Rab14, UBC12, and ATP5A levels relative to Vinculin in B. Data are presented as mean±SEM (n=3 or 4). ns: Not significant; ***: P<0.001. D: Western blot analysis of PINK1 and UBC12 in different brain regions and peripheral tissues from a 2-year-old WT monkey. Str: Striatum; Hipp: Hippocampus; Cere: cerebellum. E, F: Western blot analysis of tissues from WT monkeys (WT, 3-year-old; WT1, 1.5-year-old; WT2, 3-year-old; WT3, 3-year-old) (E) and 54-year-old human tissues (F) showing that both UBC12 and PINK1 are more abundantly expressed in primate brains compared with peripheral tissues.

relationship between PINK1 and UBC12 was selected for further study.

PINK1 deficiency reduces UBC12 expression at the protein level

To validate the observed reduction of UBC12 under PINK1-deficient conditions, additional *PINK1*-targeted monkey models were examined. In the M7 fetus—terminated at 139 days of gestation following *PINK1* targeting at the zygote stage (Yang et al., 2019)—cortical tissue exhibited decreased UBC12 expression in parallel with PINK1 loss when compared to WT newborn controls (Figure 3A, left panel). Similarly, in the 3-year-old M6 monkey, which also underwent *PINK1* targeting at fertilization, reduced UBC12 expression was observed in the substantia nigra (Figure 3A, middle panel), consistent with the findings in the M6 cortex (Figure 2B). In adult monkeys (5–10 years old) previously subjected to stereotaxic AAV CRISPR/Cas9 delivery targeting PINK1 (Han et al., 2024; Yang et al., 2022), cortical regions with PINK1 knockdown showed a corresponding reduction in UBC12 protein levels (Figure 3A, right panel). Quantitative analysis confirmed a significant decrease in UBC12 expression in PINK1-deficient samples (Figure 3B). Immunostaining was performed to compare PINK1 and UBC12 expression in injected versus non-injected regions of the monkey cortex. In non-injected areas, strong co-expression of both proteins was observed within the same cells (Figure 3C, upper panel). Quantification of integrated fluorescence intensity confirmed this co-localization (Figure 3D). In parallel, knockdown of *PINK1* in primary cultured monkey neurons led to a marked reduction in UBC12 protein levels (Figure 3E), and quantitative analysis demonstrated a significant decrease in UBC12 expression in the PINK1-deficient group (Figure 3F). This finding aligns with previous results showing that *PINK1* knockdown induces neuronal loss in cultured primate neurons (Yang et al., 2022).

To determine whether the reduction in UBC12 protein expression following *PINK1* knockdown was due to changes in transcript abundance, RT-qPCR analysis was performed using RNA from PINK1-deficient monkey brain tissues, as well as from *PINK1*-knockdown primary neurons and astrocytes. No significant differences in UBC12 mRNA expression were detected compared to controls (Figure 3G). These results suggest that PINK1 does not regulate UBC12 at the transcriptional level. Instead, evidence from multiple PINK1-deficient brain tissues and cultured neuronal cells suggests that PINK1 plays a role in stabilizing UBC12 at the protein level.

Interaction and colocalization of monkey PINK1 with UBC12

To confirm the interaction between PINK1 and UBC12, co-immunoprecipitation was performed using cortical lysates from a 7-year-old monkey. Immunoprecipitation of UBC12 resulted in the co-purification of PINK1, with higher levels of UBC12 expression correlating to increased PINK1 expression in the immunoprecipitates, supporting a physical interaction between the two proteins (Figure 4A). Consistent with this, double immunofluorescence staining of the cortex, striatum, and substantia nigra demonstrated co-expression of UBC12 and PINK1 within the same cells (Figure 4B).

To further assess their spatial association at the subcellular level, PLA analysis was performed. PLA enables *in situ* detection of PPI within cells by using oligonucleotide-linked secondary antibodies that generate a circular DNA molecule when bound in close proximity, which is subsequently amplified and visualized by fluorescence microscopy (Söderberg et al., 2008). PLA was successfully applied to the cultured monkey astrocytes to evaluate the association between endogenous PINK1 and UBC12. While individual PINK1 or UBC12 antibodies did not produce detectable fluorescent signals, their combination generated significant signals in the cytoplasm (Figure 4C). Quantification of fluorescence intensity confirmed a strong proximity signal between PINK1 and UBC12 (Figure 4D), corroborating the interaction observed in mass spectrometry and co-immunoprecipitation analyses.

Reduction of UBC12 and neddylation in PINK1-deficient monkey brains

UBC12 functions as a crucial E2-conjugating enzyme responsible for transferring NEDD8 to substrate proteins, a process known as neddylation. This modification can be detected as a series of NEDD8-positive bands on western blots (Bailly et al., 2019; Li et al., 2019). Given that impaired neddylation has been implicated in the pathogenesis of neurodegenerative diseases (Govindarajulu et al., 2022), the potential impact of PINK1 deficiency on neddylation was examined in primate brain tissue. In adult monkey cortices subjected to AAV-mediated CRISPR/Cas9 knockdown of *PINK1*, a reduction in both PINK1 and the neuronal marker NeuN were observed relative to AAV-control-injected regions (Figure 5A). Quantification of NeuN-positive cells per image (20×) showed 18±0.38 NeuN cells in the *PINK1*-knockdown brain and 58±0.72 NeuN cells in the control brain. Given that reducing PINK1 can decrease UBC12, it was necessary to establish whether diminished UBC12 is sufficient to impair NEDD8-mediated neddylation. To test this, siRNA targeting *Ubc12* was administered to the mouse brain, resulting in a pronounced reduction in NEDD8 conjugates (Figure 5B), supporting the functional role of UBC12 in maintaining NEDD8 conjugation.

In the striatum of *PINK1*-knockdown monkeys, mono-NEDD8 levels remained unchanged, while global levels of neddylated proteins were decreased (Figure 5C). These findings imply that PINK1 loss impairs NEDD8 conjugation, likely through down-regulation of UBC12, rather than limiting NEDD8 availability itself. To further establish the causal relationship between PINK1 and protein neddylation, *PINK1* knockdown was performed in primary cultured monkey neurons. As described in our previous study (Yang et al., 2022), *PINK1* knockdown not only reduced PINK1 expression and altered cell morphology (Figure 5D) but also decreased the expression of neddylated proteins in cultured monkey neurons as detected with anti-NEDD8 antibodies (Figure 5E). Moreover, comparison between the PINK1-deficient M6 monkey cortex and cultured neurons revealed that the degree of *PINK1* knockdown correlated with the reduction in neddylation (Figure 5E). Quantitative analysis of the relative levels of PINK1, UBC12, and neddylated proteins based on western blotting further supported the role of PINK1 loss in reducing UBC12 expression and neddylation (Figure 5F).

Given the primate-specific PINK1 expression (Chen et al., 2024; Yang et al., 2022), the relationship between PINK1, UBC12, and neddylation was further examined in *PINK1*-knockout mouse and pig brains to determine whether the reduction in neddylation observed in monkey brains is

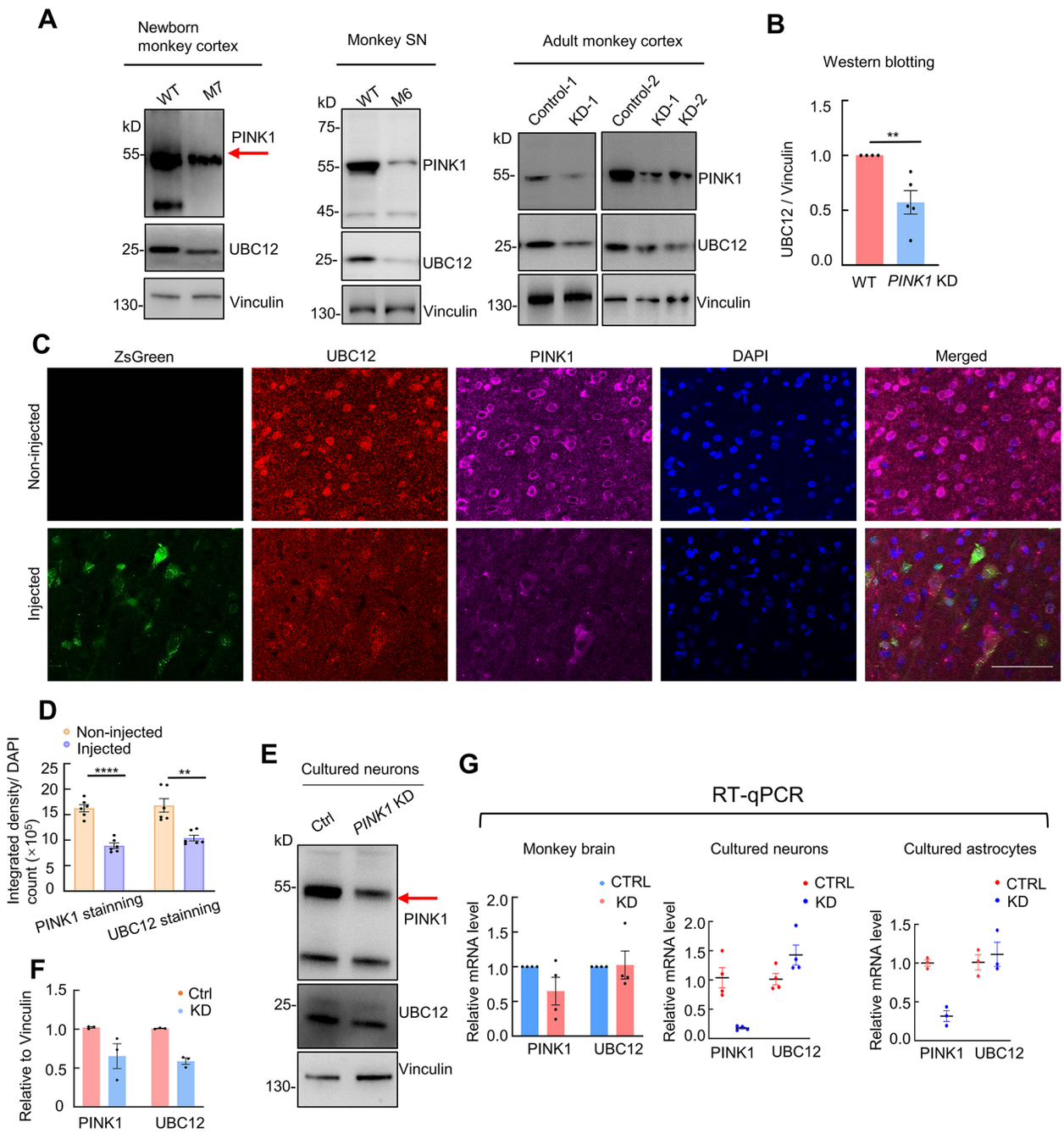

Figure 3 *PINK1* knockdown decreases UBC12 expression at the protein level

A: Western blot analysis of cortex and substantia nigra tissues from wild-type (WT) and PINK1-deficient monkeys showing that *PINK1* knockdown decreases UBC12 expression. M6 and M7 denote monkeys with embryonic PINK1 targeting (M6: 3 years; M7: aborted at E139). KD-1 and KD-2 indicate adult-onset PINK1 knockdown at 5 and 10 years of age, respectively. B: Quantification of UBC12 expression normalized to Vinculin) in panel A. Data are presented as mean±SEM (n=5). **: P<0.01. C: Double immunostaining showing reduced UBC12 expression in AAV9-*PINK1* gRNA/Cas9-injected region compared with adjacent non-infected region. Green: *PINK1* sgRNA-targeted cells; purple: PINK1 staining; red: UBC12 staining; blue: nuclear (DAPI) staining. Scale bar: 100 μm. D: Quantification of integrated fluorescence density for PINK1 and UBC12 in injected and non-injected regions. Data are presented as mean±SEM (n=6). **: P<0.01; ****: P<0.0001. E: Western blot analysis of primary cultured monkey neurons showing a reduction in PINK1 and UBC12 protein levels following PINK1 targeting. Vinculin was used as a loading control. F: Quantification of relative PINK1 and UBC12 expression in *PINK1* KD primary cultured monkey neurons. Data are presented as mean±SEM (n=3). G: Ratios of *PINK1* mRNA to *ACTB* mRNA in monkey cortex, primary cultured neurons, and astrocytes. RT-qPCR analysis showed that *PINK1* knockdown did not alter *UBC12* mRNA in monkey cortex, primary cultured neurons, or astrocytes. Brain cortical tissues of four WT and four *PINK1* mutant monkeys were used for analysis. For cultured cells, quantitative data were derived from 3–4 independent replicates. Data are presented as mean±SEM (n=3 or 4).

dependent on PINK1. In contrast to *PINK1*-knockdown monkey brains, no significant changes in UBC12 expression (Figure 5G) or in global neddylation levels detected by NEDD8 immunoblotting (Figure 5H) were observed in mouse or pig brain tissues. These findings suggest that reduced neddylation in the primate brain is specifically associated with the loss of

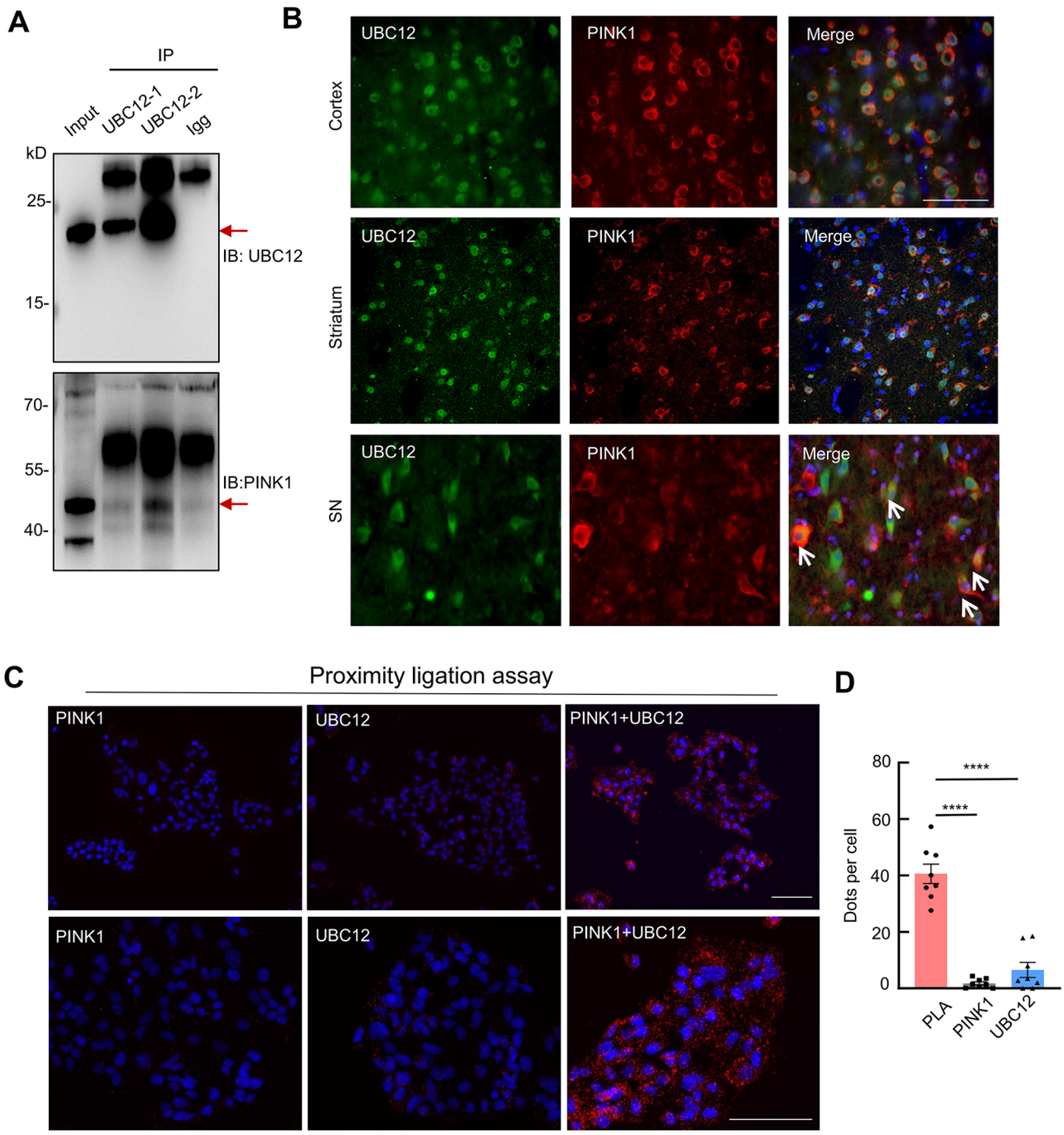

Figure 4 UBC12 interacts and colocalizes with PINK1 in the monkey brain

A: Co-immunoprecipitation using monkey brain lysates and UBC12 antibodies (lane 2, 2 μg; lane 3, 4 μg) showing an interaction between UBC12 and PINK1. IgG antibody (2 μg) served as a control (lane 4). Western blot analysis was performed using UBC12 and PINK1 antibodies. B: Co-immunostaining of PINK1 and UBC12 in the cortex, striatum, and substantia nigra of a 6-year-old monkey showing partial colocalization of PINK1 (red) and UBC12 (green). Nuclei were counterstained with DAPI. Scale bar: 100 μm. C: Proximity ligation assay (PLA) in primary cultured monkey astrocytes between PINK1 and UBC12, and with PINK1 or UBC12 antibodies alone. Red fluorescence in monkey astrocytes indicates PINK1-UBC12 interactions. Nuclei were counterstained with DAPI (blue). Scale bar: 50 μm. D: Quantification of PLA signal (red dots per cell). Data are presented as mean±SEM. *n*=8 sections for each group. ****: *P*< 0.0001.

PINK1, likely through its regulation of UBC12 stability. This primate-specific regulatory axis may contribute to neurodegeneration under conditions of PINK1 deficiency (Figure 6).

DISCUSSION

PINK1 has long been implicated in mitophagy, primarily through *in vitro* studies involving acute mitochondrial injury; however, *in vivo* validation has been limited due to the near absence of detectable PINK1 expression in rodent models and most cultured cells under normal physiological conditions (Akundi et al., 2011; Gispert et al., 2009; Pickrell & Youle, 2015). Our recent work demonstrated that PINK1 is selectively expressed in the primate brain (Yang et al., 2019, 2022),

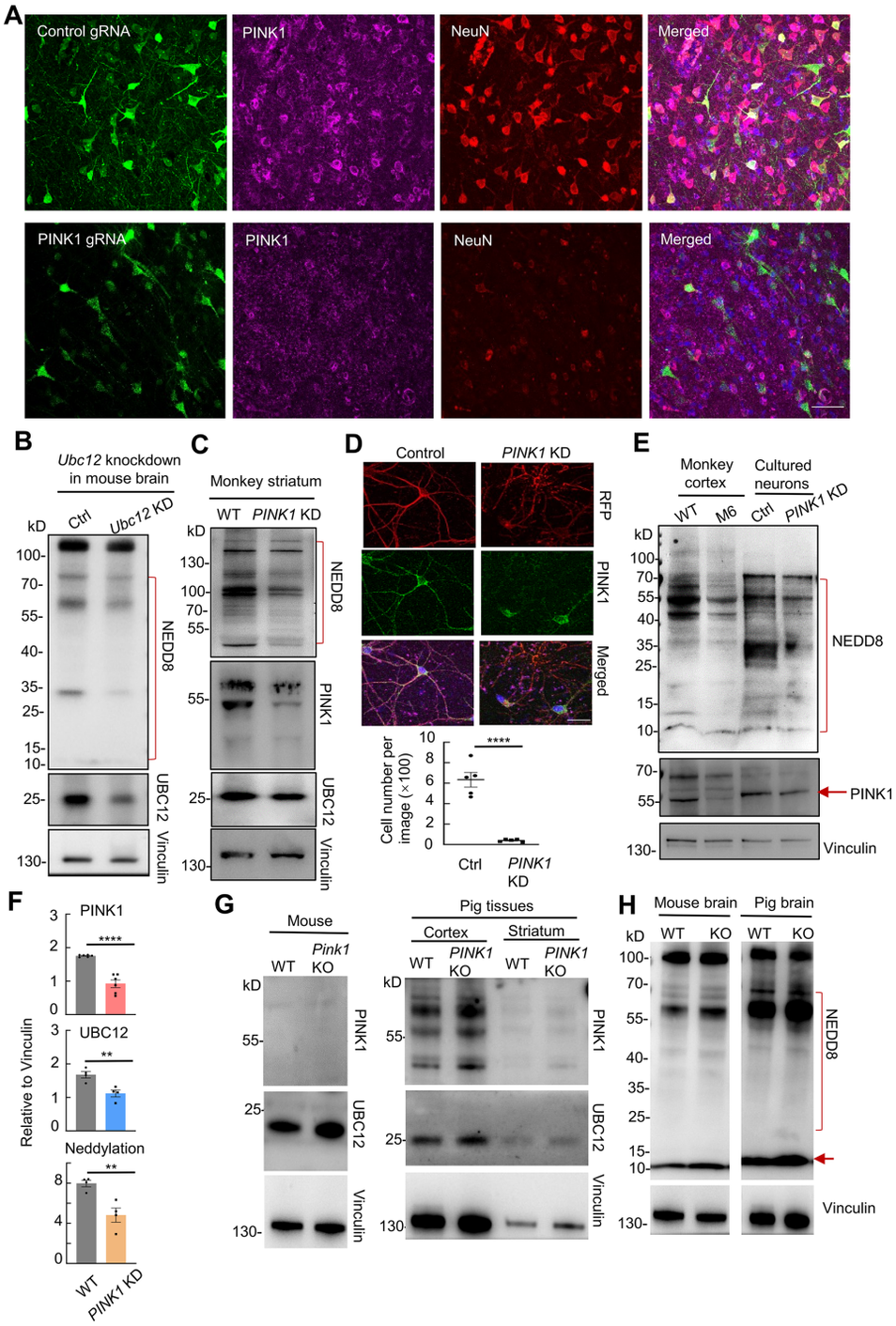

Figure 5 PINK1 deficiency selectively reduces UBC12 expression and neddylated proteins in the monkey brain

A: Double immunostaining showing reduced NeuN expression in the AAV9-*PINK1* gRNA/Cas9-injected region compared with the control gRNA/Cas9 injected-region. Green: *PINK1* sgRNA-targeted cells; purple: PINK1 staining; red: NeuN staining; blue: nuclear (DAPI) staining. Scale bar: 50 μm. B: Western blot analysis of mouse brain lysates showing reduced UBC12 and NEDD8-neddylated proteins following *Ubc12* knockdown. C: Western blot analysis showing that PINK1 deficiency reduced UBC12 and NEDD8 expression in the monkey striatum (WT: 3-year-old; M6: *PINK1* mutant, 3-year-old). D: Immunostaining showing axonal degeneration *in PINK1*-targeted monkey neurons. Green: PINK1 staining; red: *PINK1* sgRNA-targeted cells; blue: nuclear (DAPI) staining. Scale bar: 10 μm. Quantification of neuronal cell numbers per image is shown below. Data are presented as mean±SEM. (*n*=5 sections per group). ****: *P*<0.0001. E: Western blot analysis showing that PINK1 loss reduced NEDD8-neddylated protein expression in the monkey cortex (WT: 3-year-old; M6: *PINK1* mutant, 3-year-old) and primary cultured monkey neurons. F: Quantification of PINK1, UBC12, and NEDD8 in wild-type (WT) and *PINK1*-knockdown monkey brain tissues and neurons. Vinculin served as the loading control. Data are presented as mean±SEM. (*n*=6 for PINK1 quantification, *n*=4 for UBC12 and NEDD8 quantification). **: *P*<0.01; ****: *P*<0.0001. G: Western blot analysis of brain cortex tissues from *Pink1* knockout and WT mice (left panel). Western blot analysis of brain tissues from *PINK1* knockout and WT pigs (right panel). UBC12 protein expression remained unchanged in the brain tissues of *PINK1* knockout mice and pigs. H: Western blot analysis of NEDD8-neddylated proteins in the brain tissues of *PINK1* knockout mice and pigs. Red arrow represents NEDD8 monomer.

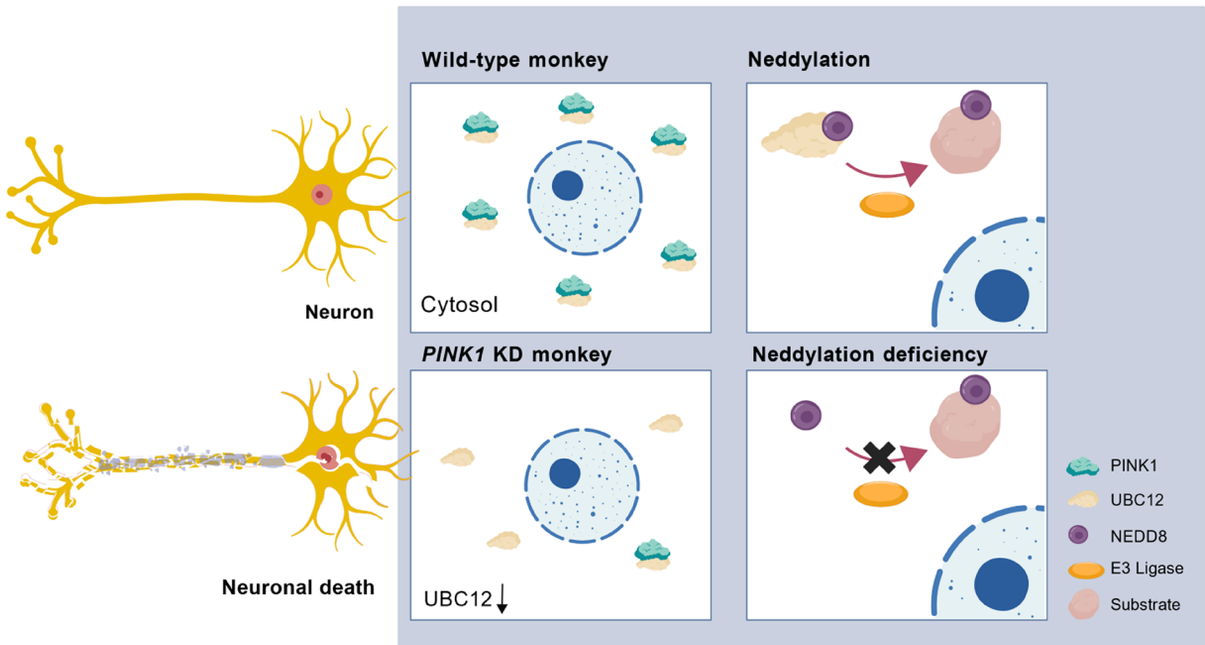

Figure 6 Proposed model of *PINK1* knockdown-induced neuronal death

PINK1 knockdown in the monkey brain reduces UBC12 expression, leading to decreased cellular neddylation, which may contribute to neuronal death. The schematic was generated using BioGDP.com (Jiang et al., 2025).

providing a platform to examine its endogenous function *in vivo*. In the present study, PINK1 was found to interact with and co-localize alongside the ubiquitin-conjugating enzyme UBC12 in the monkey brain, and knockdown of *PINK1* markedly reduced UBC12 protein abundance. This reduction was accompanied by decreased global neddylation, implicating a mechanistic link between PINK1 and the neddylation pathway in primate.

Neddylation, a ubiquitin-like post-translational modification, regulates key aspects of cellular homeostasis and viability, comparable in importance to phosphorylation and ubiquitylation (Ramazi & Zahiri, 2021; Zhang et al., 2024). This process involves the attachment of NEDD8 to a lysine residue on a substrate protein, facilitated by a three-step enzymatic cascade involving the E1 NEDD8-activating enzyme (NAE), NEDD8-conjugating enzyme E2, and substrate-specific NEDD8-E3 ligases (Kamitani et al., 1997; Rabut & Peter, 2008). Similar to ubiquitin, NEDD8 is activated via ATP-dependent adenylation (Walden et al., 2003), transferred to UBE2M (also known as UBC12) or UBE2F, two recognized E2 enzymes, via a trans-thiolation reaction (Huang et al., 2005, 2009), and ultimately conjugated to target proteins via E3 ligases (Zhou et al., 2018).

CRISPR/Cas9-mediated *PINK1* knockdown in the monkey brain revealed a previously unrecognized regulatory role for PINK1 in maintaining neddylation homeostasis. PINK1 deficiency selectively reduced UBC12 at the protein level without affecting its transcript expression, indicating post-transcriptional control. PINK1 deficiency led to reduced UBC12 protein levels, which, in turn, disrupted NEDD8 conjugation and caused a global decline in protein neddylation. This regulatory effect was specific to the primate brain, as no comparable changes in UBC12 abundance or neddylation were observed in *PINK1*-knockout mouse or pig brains, where endogenous PINK1 is nearly undetectable. These findings suggest that primate-restricted expression of PINK1 modulates neddylation through stabilization of UBC12, with potential implications for neural function. Impaired neddylation has been linked to neurodegenerative processes, including Parkinson's disease, where abnormal NEDD8 accumulation has been detected in Lewy bodies and defective NEDD8 modification has been implicated in disease pathogenesis (Chen et al., 2012; Choo et al., 2012; Dil Kuazi et al., 2003; Govindarajulu et al., 2022; Mori et al., 2005; Saurat et al., 2024; Um et al., 2012; Zhang et al., 2024).

Collectively, the findings from this study suggest that PINK1 plays a role in regulating neddylation under physiological conditions. Considering the importance of neddylation in various cellular processes, such as neurodegeneration and tumorigenesis (Zhang et al., 2024), and the specific expression of PINK1 in the primate brain, these results reveal broader functions for PINK1 in NHPs and establish a new framework for exploring its roles beyond mitophagy.

Limitations of the study

Several study limitations require further investigation. Although PINK1 deficiency did not alter *UBC12* transcript levels, the observed reduction in UBC12 protein suggests that PINK1 may regulate its stability through direct interaction or phosphorylation. Elucidating the mechanism by which PINK1 stabilizes UBC12, including identifying the relevant binding domains, will require further study. In addition, given the diverse array of neddylated proteins, it will be essential to employ substrate-specific antibodies in the monkey brain to determine whether PINK1 influences the modification of defined targets within the neddylation pathway.

SUPPLEMENTARY DATA

Supplementary data to this article can be found online.

COMPETING INTERESTS

The authors declare that they have no competing interests.

AUTHORS' CONTRIBUTIONS

W.L.Y. designed and supervised the research experiments. W.H., T.X.,

G.K.Z., Y.X.L., C.Z.L., X.S.C., T.Z., L.J., Y.T.L., X.X., X.Y.L. performed the molecular biology experiments and pathological studies. W.L.Y. and X.J.L. wrote the manuscript, S.H.L. and X.Y.G. edited the manuscript. All authors read and approved the final version of the manuscript.

ACKNOWLEDGMENTS

We thank Prof. Jian-Guo Zhao from the Institute of Zoology, Chinese Academy of Sciences, for providing WT and age-matched *PINK1* knockout pig tissues. We thank Guangzhou and Guangdong Landao Biotechnology Co. Ltd, Guangzhou, for providing animal facility and care.

REFERENCES

Akundi RS, Huang ZY, Eason J, et al. 2011. Increased mitochondrial calcium sensitivity and abnormal expression of innate immunity genes precede dopaminergic defects in Pink1-deficient mice. *PLoS One*, **6**(1): e16038.

Arena G, Valente EM. 2017. PINK1 in the limelight: multiple functions of an eclectic protein in human health and disease. *The Journal of Pathology*, **241**(2): 251–263.

Ayuso-García P, Sánchez-Rueda A, Velasco-Avilés S, et al. 2024. Neddylation orchestrates the complex transcriptional and posttranscriptional program that drives Schwann cell myelination. *Science Advances*, **10**(15): eadm7600.

Bailly AP, Perrin A, Serrano-Macia M, et al. 2019. The balance between mono- and NEDD8-chains controlled by NEDP1 upon DNA damage is a regulatory module of the HSP70 ATPase activity. *Cell Reports*, **29**(1): 212–224. e8.

Beilina A, Van Der Brug M, Ahmad R, et al. 2005. Mutations in PTEN-induced putative kinase 1 associated with recessive parkinsonism have differential effects on protein stability. *Proceedings of the National Academy of Sciences of the United States of America*, **102**(16): 5703–5708.

Chen XS, Han R, Liu YT, et al. 2024. Comparative analysis of primate and pig cells reveals primate-specific PINK1 expression and phosphorylation. *Zoological Research*, **45**(2): 242–252.

Chen YZ, Neve RL, Liu H. 2012. Neddylation dysfunction in Alzheimer's disease. *Journal of Cellular and Molecular Medicine*, **16**(11): 2583–2591.

Chen ZZ, Wang JY, Kang Y, et al. 2021. *PINK1* gene mutation by pair truncated sgRNA/Cas9-D10A in cynomolgus monkeys. *Zoological Research*, **42**(4): 469–477.

Choo YS, Vogler G, Wang D, et al. 2012. Regulation of parkin and PINK1 by neddylation. *Human Molecular Genetics*, **21**(11): 2514–2523.

Chu CT. 2019. Multiple pathways for mitophagy: a neurodegenerative conundrum for Parkinson's disease. *Neuroscience Letters*, **697**: 66–71.

de Vries RLA, Przedborski S. 2013. Mitophagy and Parkinson's disease: be eaten to stay healthy. *Molecular and Cellular Neuroscience*, **55**: 37–43.

Dil Kuazi A, Kito K, Abe Y, et al. 2003. NEDD8 protein is involved in ubiquitinated inclusion bodies. *The Journal of Pathology*, **199**(2): 259–266.

Eldeeb MA, Ragheb MA. 2020. *N*-degron-mediated degradation and regulation of mitochondrial PINK1 kinase. *Current Genetics*, **66**(4): 693–701.

Enchev RI, Schulman BA, Peter M. 2015. Protein neddylation: beyond cullin–RING ligases. *Nature Reviews Molecular Cell Biology*, **16**(1): 30–44.

Gispert S, Ricciardi F, Kurz A, et al. 2009. Parkinson phenotype in aged PINK1-deficient mice is accompanied by progressive mitochondrial dysfunction in absence of neurodegeneration. *PLoS One*, **4**(6): e5777.

Gladkova C, Maslen SL, Skehel JM, et al. 2018. Mechanism of parkin activation by PINK1. *Nature*, **559**(7714): 410–414.

Govindarajulu M, Ramesh S, Shankar T, et al. 2022. Role of neddylation in neurodegenerative diseases. *NeuroSci*, **3**(4): 533–545.

Greene AW, Grenier K, Aguileta MA, et al. 2012. Mitochondrial processing peptidase regulates PINK1 processing, import and Parkin recruitment. *EMBO Reports*, **13**(4): 378–385.

Han R, Wang Q, Xiong X, et al. 2024. Deficiency of parkin causes neurodegeneration and accumulation of pathological α-synuclein in monkey models. *The Journal of Clinical Investigation*, **134**(20): e179633.

Huang DT, Ayrault O, Hunt HW, et al. 2009. E2-RING expansion of the NEDD8 cascade confers specificity to cullin modification. *Molecular Cell*, **33**(4): 483–495.

Huang DT, Paydar A, Zhuang M, et al. 2005. Structural basis for recruitment of Ubc12 by an E2 binding domain in NEDD8's E1. *Molecular Cell*, **17**(3): 341–350.

Jiang S, Li HQ, Zhang LWY, et al. 2025. Generic Diagramming Platform (GDP): a comprehensive database of high-quality biomedical graphics. *Nucleic Acids Research*, **53**(D1): D1670–D1676.

Kamitani T, Kito K, Nguyen HP, et al. 1997. Characterization of NEDD8, a developmentally down-regulated ubiquitin-like protein. *Journal of Biological Chemistry*, **272**(45): 28557–28562.

Kane LA, Lazarou M, Fogel AI, et al. 2014. PINK1 phosphorylates ubiquitin to activate Parkin E3 ubiquitin ligase activity. *Journal of Cell Biology*, **205**(2): 143–153.

Kitada T, Pisani A, Porter DR, et al. 2007. Impaired dopamine release and synaptic plasticity in the striatum of *PINK1*-deficient mice. *Proceedings of the National Academy of Sciences of the United States of America*, **104**(27): 11441–11446.

Koyano F, Okatsu K, Kosako H, et al. 2014. Ubiquitin is phosphorylated by PINK1 to activate parkin. *Nature*, **510**(7503): 162–166.

Li LH, Kang JH, Zhang WJ, et al. 2019. Validation of NEDD8-conjugating enzyme UBC12 as a new therapeutic target in lung cancer. *eBioMedicine*, **45**: 81–91.

Liu DQ, Che XY, Wu GZ. 2024. Deciphering the role of neddylation in tumor microenvironment modulation: common outcome of multiple signaling pathways. *Biomarker Research*, **12**(1): 5.

Liu Y, Lear TB, Verma M, et al. 2020. Chemical inhibition of FBXO7 reduces inflammation and confers neuroprotection by stabilizing the mitochondrial kinase PINK1. *JCI Insight*, **5**(11): e131834.

Liu YT, Huang W, Wen JY, et al. 2025. Differential distribution of PINK1 and Parkin in the primate brain implies distinct roles. *Neural Regeneration Research*, **20**(4): 1124–1134.

McWilliams TG, Prescott AR, Montava-Garriga L, et al. 2018. Basal mitophagy occurs independently of PINK1 in mouse tissues of high metabolic demand. *Cell Metabolism*, **27**(2): 439–449. e5.

Mori F, Nishie M, Piao YS, et al. 2005. Accumulation of NEDD8 in neuronal and glial inclusions of neurodegenerative disorders. *Neuropathology and Applied Neurobiology*, **31**(1): 53–61.

Narendra DP, Jin SM, Tanaka A, et al. 2010. PINK1 is selectively stabilized on impaired mitochondria to activate Parkin. *PLoS Biology*, **8**(1): e1000298.

O'Flanagan CH, O'Neill C. 2014. PINK1 signalling in cancer biology. *Biochimica et Biophysica Acta (BBA)-Reviews on Cancer*, **1846**(2): 590–598.

Pickrell AM, Huang CH, Kennedy SR, et al. 2015. Endogenous Parkin preserves dopaminergic substantia nigral neurons following mitochondrial DNA mutagenic stress. *Neuron*, **87**(2): 371–381.

Pickrell AM, Youle RJ. 2015. The roles of PINK1, parkin, and mitochondrial fidelity in Parkinson's disease. *Neuron*, **85**(2): 257–273.

Rabut G, Peter M. 2008. Function and regulation of protein neddylation. *EMBO Reports*, **9**(10): 969–976.

Ramazi S, Zahiri J. 2021. Post-translational modifications in proteins: resources, tools and prediction methods. *Database*, **2021**: baab012.

Saurat N, Minotti AP, Rahman MT, et al. 2024. Genome-wide CRISPR screen identifies neddylation as a regulator of neuronal aging and AD neurodegeneration. *Cell Stem Cell*, **31**(8): 1162–1174. e8.

Söderberg O, Leuchowius KJ, Gullberg M, et al. 2008. Characterizing

proteins and their interactions in cells and tissues using the *in situ* proximity ligation assay. *Methods*, **45**(3): 227–232.

Tu ZC, Yang WL, Yan S, et al. 2017. Promoting Cas9 degradation reduces mosaic mutations in non-human primate embryos. *Scientific Reports*, **7**(1): 42081.

Um JW, Han KA, Im E, et al. 2012. Neddylation positively regulates the ubiquitin E3 ligase activity of parkin. *Journal of Neuroscience Research*, **90**(5): 1030–1042.

Vogl AM, Brockmann MM, Giusti SA, et al. 2015. Neddylation inhibition impairs spine development, destabilizes synapses and deteriorates cognition. *Nature Neuroscience*, **18**(2): 239–251.

Walden H, Podgorski MS, Huang DT, et al. 2003. The structure of the APPBP1-UBA3-NEDD8-ATP complex reveals the basis for selective ubiquitin-like protein activation by an E1. *Molecular Cell*, **12**(6): 1427–1437.

Wang XL, Cao CW, Huang JJ, et al. 2016. One-step generation of triple gene-targeted pigs using CRISPR/Cas9 system. *Scientific Reports*, **6**(1): 20620.

Wang ZT, Chan SW, Zhao H, et al. 2023. Outlook of PINK1/Parkin signaling in molecular etiology of Parkinson's disease, with insights into *Pink1* knockout models. *Zoological Research*, **44**(3): 559–576.

Xiong H, Wang DL, Chen LN, et al. 2009. Parkin, PINK1, and DJ-1 form a ubiquitin E3 ligase complex promoting unfolded protein degradation. *The Journal of Clinical Investigation*, **119**(3): 650–660.

Yamano K, Youle RJ. 2013. PINK1 is degraded through the N-end rule pathway. *Autophagy*, **9**(11): 1758–1769.

Yang WL, Guo XY, Tu ZC, et al. 2022. PINK1 kinase dysfunction triggers neurodegeneration in the primate brain without impacting mitochondrial homeostasis. *Protein & Cell*, **13**(1): 26–46.

Yang WL, Liu YB, Tu ZC, et al. 2019. CRISPR/Cas9-mediated *PINK1* deletion leads to neurodegeneration in rhesus monkeys. *Cell Research*, **29**(4): 334–336.

Yang WL, Wang GH, Wang CE, et al. 2015. Mutant alpha-synuclein causes age-dependent neuropathology in monkey brain. *Journal of Neuroscience*, **35**(21): 8345–8358.

Zhang SZ, Yu Q, Li ZJ, et al. 2024. Protein neddylation and its role in health and diseases. *Signal Transduction and Targeted Therapy*, **9**(1): 85.

Zheng YC, Guo YJ, Wang B, et al. 2021. Targeting neddylation E2s: a novel therapeutic strategy in cancer. *Journal of Hematology & Oncology*, **14**(1): 57.

Zhou LS, Zhang WJ, Sun Y, et al. 2018. Protein neddylation and its alterations in human cancers for targeted therapy. *Cellular Signalling*, **44**: 92–102.

Zhou XQ, Xin JG, Fan NN, et al. 2015. Generation of CRISPR/Cas9-mediated gene-targeted pigs via somatic cell nuclear transfer. *Cellular and Molecular Life Sciences*, **72**(6): 1175–1184.